encapsulated in interconnected carbon nanospheres due to that the inner hematite cores can be reduced to magnetite by the outer carbon layers (Fig. 1A). The source materials and the synthetic processes are both viable for large-scale production, making this approach particularly attractive for practical applications.

The crystallographic structure, morphology and microstructure of the hydrothermal product (Fe_2O_3@C nanospheres) are determined by XRD, SEM and TEM, as shown in Fig. 2. From XRD pattern of Fig. 2(a), we can see that all of the diffraction peaks could be indexed to the rhombohedral phase of hematite (α-Fe_2O_3) (JCPDS No. 33-0664) and the broadness of the diffraction peaks indicates the small size and not well crystallized feature of the Fe_2O_3 nanocrystals. According the Scherrer's formula, the average crystallite size of the Fe_2O_3 phase is found to be ~3.8 nm. The broad signal in the range of 20–30° may be due to the presence of non-crystalline carbon in the hydrothermal product, because the most intense reflection for graphitic carbon (002 layer) should appear at about 26.8°.

Fig. 2(b) shows a typical SEM image of the hydrothermal product. It can be observed that this sample exhibits spherical nanoparticles with an average diameter of ~65 nm and a narrow size distribution. A closer examination revealed that a majority of these nanospheres is interconnected, resulting in porous self-assembled structure with rough surface. In order to unveil the microstructure of these nanospheres, the sample was characterized by TEM, as shown in Fig. 2(c–d). A low-magnification TEM image in Fig. 2(c) presents that the nanospheres, which exhibit an apparent core–shell nanostructure, are indeed interconnected. A high-magnification TEM image of Fig. 2(d) reveals that the outer carbon layer with a thickness of 5–15 nm is amorphous, and the inner hematite core is actually composed of dozens of tiny Fe_2O_3 nanocrystals with a size of ~4 nm, in agreement with above XRD result.

The interconnected characteristic of Fe_2O_3@C nanospheres enable their composition of individual components to be varied without damaging the overall structure. By careful annealing at 500 °C for 2 h in Ar, Fe_3O_4@C nanospheres can be derived through phase transformation of Fe_2O_3 to Fe_3O_4, which was confirmed by the color variation from brown to totally black and the strong ferromagnetism of the final black products after annealing, and the following XRD analysis and TEM observations. The XRD pattern (Fig. 2(a)) of the Fe_3O_4@C nanospheres exhibits diffraction peaks of Fe_3O_4 nanocrystals which matched very well with those of magnetite (JCPDS No. 19-0629). The strong diffraction peaks indicate good crystallinity of the Fe_3O_4 phase. The average particle size of Fe_3O_4 nanocrystals calculated from the largest diffraction peak (311) by using the Scherrer's formula is estimated to ~9.14 nm. However, no diffraction peak of graphite was detected in the XRD pattern, indicating the not well crystallized nature of the carbon layer.

Typical SEM and TEM images provide insight into the morphology and microstructure of the final product (Fe_3O_4@C nanospheres). Fig. 3(a) displays a typical SEM image of nanospheres prepared by calcinating Fe_2O_3@C nanospheres at 500 °C for 2 h under Ar. The spheres are uniform and interconnected, virtually indistinguishable from Fe_2O_3@C nanospheres prepared by hydrothermal reaction, except for the slight decrease of roughness and diameter because of the reduction of Fe_2O_3 to Fe_3O_4 by the outer carbon layer during the thermal treatment process. Importantly, it should be noted that the interconnected structure of the Fe_3O_4@C nanospheres is favorable for achieving high durability and high rate capability when used as a LIB anode [25]. Fig. 3(b–d) show TEM images of the Fe_3O_4@C nanospheres, which further verify the

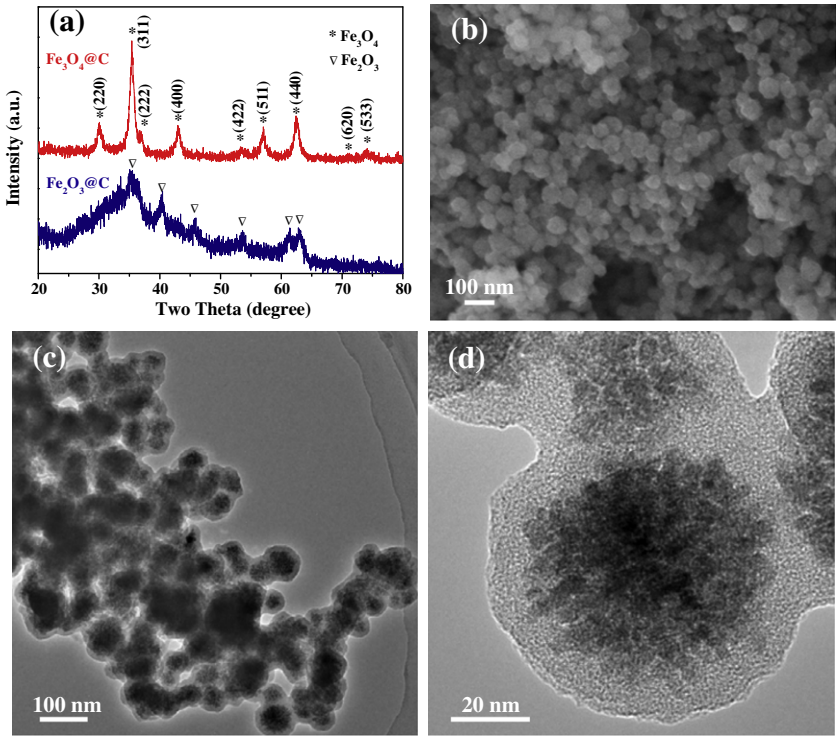

Fig. 2 – (a) XRD patterns of the Fe_2O_3@C and Fe_3O_4@C nanospheres. (b–d) SEM and TEM images of the Fe_2O_3@C nanospheres.